Sensorless Position Measurement in Synchronous Reluctance Motor

M. S. Arefeen, *Student Member, IEEE,* M. Ehsani, *Senior Member, IEEE,* and T. A. Lipo, *Fellow, IEEE*

***Abstract*—A new discrete position sensor elimination technique for a sinusoidally wound synchronous reluctance motor drive is presented. The proposed technique determines the rotor position at zero crossing of the phase currents. The rotor position between the zero crossings is determined by applying extrapolation. The proposed technique works well at all speeds, including zero speed. This technique can be used in both vector controlled and conventional constant Volts/Hertz type of motor controllers.**

I. Introduction

SYNCHRONOUS reluctance motor (SynRM) drives have recently received renewed attention [1]. This interest is mainly due to modern field oriented control strategies, which have recently been applied to these motors [2]–[5]. In particular, it has been shown that a properly designed and field oriented SynRM can perform as well as an induction motor drive when the field weakening range is not too wide [3], [7], [6]. However, the inherent characteristics of the SynRM make it preferable for some applications. Some of the desirable characteristics are as follows [2]:

1) The stator of the SynRM is constructed from a cylindrical structure identical to an induction motor. Hence the stator of both machines can be constructed from the same assembly line.
2) No starting cage is necessary with an inverter supply. The rotor can therefore be designed purely for synchronous performance.
3) Electronic control makes the motor auto-synchronous and can assure an optimum torque angle at all loads and torques, consequently giving the motor a very high pullout torque.
4) No damping winding is necessary. This makes it possible to design the motor for the highest reluctance difference $X_d - X_q$, thereby increasing the power density of the machine.
5) The torque pulsations and the acoustic problem are not as severe as those for variable reluctance machines.
6) Vector control techniques can be applied in order to achieve high performance.

However, field orientation control of SynRM requires position sensor information as is common for all ac machines. However, a discrete position sensor reduces the reliability and ruggedness of the drive and increases its cost. The SynRM however possess unique features which make position sensing much simpler and reliable than either conventional squirrel cage induction machines or variable reluctance machines. In contrast to induction machine the SynRM possess saliency which permits the rotor position to be sensed since the inductance per phase is a function of rotor position. This allows sensing position at zero speed which is impossible for an induction machine. Secondly, in contrast to the variable reluctance motor, the stator windings of the SynRM are magnetically coupled. Hence, voltages are induced in the stator winding upon open circuit of a phase, which allows sensing of the emf. These two features in combination make the task of sensing position easier than for either an induction or variable reluctance motor. A new indirect rotor position sensing technique for SynRM, utilizing only the input variables (voltages and phase currents) and the rotor saliency information, is presented in this paper.

Manuscript received April 22, 1993; revised June 9, 1994.

M. S. Arefeen and M. Ehsani are with the Power Electronics Laboratory, Department of Electrical Engineering, Texas A&M University, College Station, TX 77843 USA.

T. A. Lipo is with the Department of Electrical & Computer Engineering, University of Wisconsin–Madison, Madison, WI 53706 USA.

IEEE Log Number 9405306.

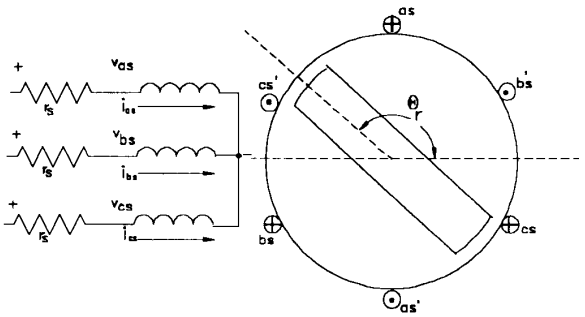

Fig. 1. Equivalent circuit of a two-pole SynRM.

II. Equivalent Circuit

For purposes of analysis, a two-pole, three-phase wye connected SynRM is considered as shown in Fig. 1. The performance of the SynRM can be described by the equations given below,

$$V_{as} = r_s i_{as} + \frac{d}{dt}(\lambda_{as}) \tag{1}$$

$$V_{bs} = r_s i_{bs} + \frac{d}{dt}(\lambda_{bs}) \tag{2}$$

$$V_{cs} = r_s i_{cs} + \frac{d}{dt}(\lambda_{cs}) \tag{3}$$

where, v_{as}, v_{bs}, and v_{cs} are the applied terminal voltages, r_s is the stator winding resistance and λ_{as}, λ_{bs}, and λ_{cs} are the

flux linkages of the individual phases. The flux linkages can be expressed as,

$$\lambda_{as} = L_{aa}i_{as} + L_{ab}i_{bs} + L_{ac}i_{cs} \tag{4}$$

$$\lambda_{bs} = L_{ab}i_{as} + L_{bb}i_{bs} + L_{bc}i_{cs} \tag{5}$$

$$\lambda_{cs} = L_{ca}i_{as} + L_{bc}i_{bs} + L_{cc}i_{cs} \tag{6}$$

where the self and the mutual inductances of the machine can be written as, [8]

$$L_{aa} = L_{ls} + L_A - L_B \cos 2\theta_r \tag{7}$$

$$L_{bb} = L_{ls} + L_A - L_B \cos 2\left(\theta_r - \frac{2\pi}{3}\right) \tag{8}$$

$$L_{cc} = L_{ls} + L_A - L_B \cos 2\left(\theta_r + \frac{2\pi}{3}\right) \tag{9}$$

$$L_{ab} = -\frac{1}{2}L_A - L_B \cos 2\left(\theta_r - \frac{\pi}{3}\right) \tag{10}$$

$$L_{ac} = -\frac{1}{2}L_A - L_B \cos 2\left(\theta_r + \frac{\pi}{3}\right) \tag{11}$$

$$L_{bc} = -\frac{1}{2}L_A - L_B \cos 2(\theta_r + \pi) \tag{12}$$

where, $L_{mq} = 3/2(L_A - L_B)$ and $L_{md} = 3/2(L_A + L_B)$. Equations (4) through (6) show the coupling between different phases and (7) through (12) show the dependence of the mutual and self inductances on the rotor position, θr. The proposed technique utilizes these facts to determine the rotor position as described in the following section.

III. The Proposed Technique

The rotor position information embedded in the SynRM equations above will be obtained by employing a special switching technique for the current regulated pulsewidth modulated (CRPWM) converter. In a regular CRPWM converter the phase switches are normally turned on and off in order to make the individual phase currents follow the desired reference within a desired band. However, in the modified switching technique, both the switches of that phase are turned off when the current of a particular phase; e.g., phase A crosses zero. The remaining two phases (in this case phases B and C) are excited in series by turning on alternate pairs of switches (the lower switch of phase B and the upper switch of phase C (see Fig. 2(a)) or the lower switch of phase C and the upper switch of phase B (Fig. 2b)). This modified switching pattern will extend the zero crossing interval of phase A for a short interval. The currents in phases B and C can be controlled to follow a constant reference during this period. The description of this constant reference PWM of the phases B and C is explained later with simulation results. Although current of phase A during this extended zero crossing period will be zero, a voltage will be induced in phase A due to the currents in other two phases, which can be obtained by setting $i_{as} = 0$ in (1) in which case,

$$V_{\text{ind}} = \frac{d}{dt}(L_{ab}i_{bs} + L_{ac}i_{cs}). \tag{13}$$

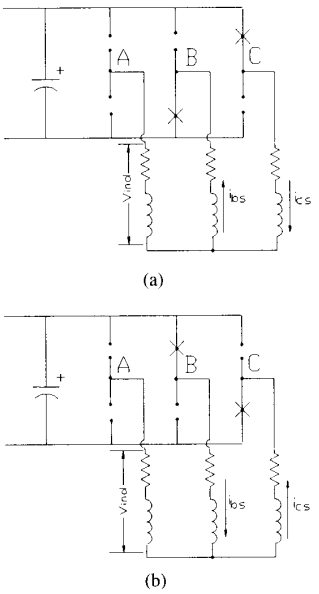

Fig. 2. Circuit configurations during the extension of the zero crossing period of phase A current.

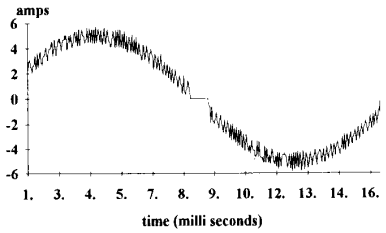

Fig. 3. Extension of the zero crossing period of phase A current.

Since phase B and phase C are now effectively in series, $i_{bs} = -i_{cs}$ and $d/dt(i_{bs}) = -d/dt(i_{cs})$ and the (13) becomes,

$$V_{\text{ind}} = (L_{ab} - L_{ac})\frac{d}{dt}i_{bs} + i_{bs}\frac{d}{dt}(L_{ab} - L_{ac}). \tag{14}$$

Using (10) and (11), the induced voltage can consequently be written as,

$$V_{\text{ind}} = K_1 \sin(2\theta_r) + K_2 \cos(2\theta_r) \tag{15}$$

where,

$$K_1 = -\left(2L_B \sin\frac{2\pi}{3}\right)\frac{d}{dt}i_{bs}$$

$$K_2 = -\left(4L_B\omega_r \sin\frac{2\pi}{3}\right)i_{bs}.$$

In (15), ω_r is the rotor speed in hertz, which is equal to the frequency applied to the stator divided by the number of pole pairs. Thus, by knowing the induced voltage V_{ind}, the slope and the instantaneous value of the current i_{bs} and using ω_r, it is theoretically possible to compute instantaneous value of the rotor position θ_r.

Fig. 3 shows a trace of the phase A current of a simulated SynRM drive wherein the zero crossing period of the phase

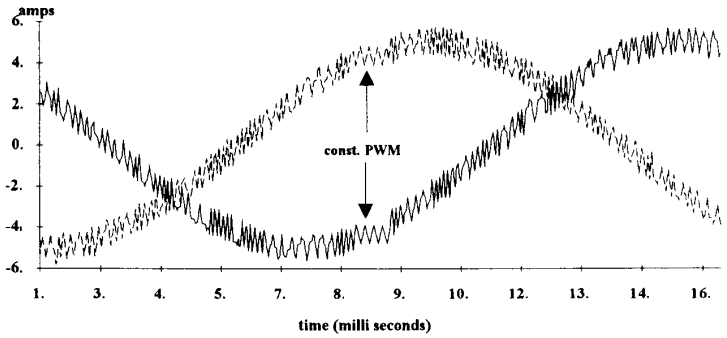

Fig. 4. Phase B and phase C current go into constant PWM during the extended zero crossing period of phase A.

A current is extended by applying the proposed technique. During the extended zero crossing period of phase A current, phases B and C of the converter are switched in a special diagnostic manner for a short interval. This diagnostic switching interval consists of following a constant reference current, in each phase, by means of hysteresis control. The level of the constant reference currents in phases B and C are exactly the instantaneous values of these currents, respectively, at the instant of phase A current zero crossing, as shown in Fig. 4.

During this diagnostic PWM interval, the instantaneous slopes and the magnitudes of phases B and C currents become equal and opposite. The voltage induced in phase A due to the currents flowing through phases B and C is shown in Fig. 5. The sequence of coupled voltage pulses, shown in Fig. 5, have the instantaneous rotor angle encoded in their amplitudes, according to (15). Each individual pulse amplitude sample can deliver one rotor angle sample by use of a look-up table. The table contains the inverse function of (15), solved for θ_r, in discrete form. Thus, several samples of the rotor angle are obtained during each diagnostic PWM interval. These samples can be used for two purposes. The multiple samples can be used in an error reduction and noise elimination algorithm. The change of θ_r from sample to sample can also be used to enhance speed and rotor angle extrapolation algorithms between two zero crossings when the change of speed is very high, such as during start-up. It should also be mentioned that the mathematical analysis ((4) through (12)) is only used to show the feasibility of the proposed technique. In practice the actual measurements of voltages, currents, rotor angles, etc., from the motor are used to create the look-up table. Thus, the nonideal variations, of the actual machine parameters, from the theory will be accounted for in the look-up table.

Although the proposed technique has been described only for phase A, the same technique can clearly be applied for phases B and C. Thus, for the six zero crossings within one electrical cycle of a three-phase machine this technique gives six rotor position measurements. Therefore, extrapolation technique has to be applied in order to estimate rotor positions between two zero crossings. A linear extrapolation will be sufficient to estimate rotor positions during the constant speed operation of the drive. But, during the acceleration period of the drive, linear extrapolation will introduce errors in rotor

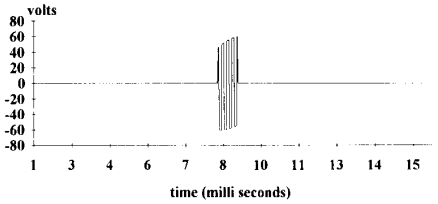

Fig. 5. Phase induced voltage during the constant PWM of phase B and phase C.

position estimation. Thus, acceleration of the drive has to be limited, so that the rotor estimation error between two zero crossings does not exceed a predefined error margin [10]. If the individual sample error $\Delta\theta_{\text{sample}}$ at each zero crossings, is taken as the acceptable margin of error for extrapolation between two zero crossings, then the acceleration, a, of the drive is limited by,

$$a \leq 72 \cdot \Delta\theta_{\text{sample}} \cdot f_e^2 \tag{16}$$

where, f_e is the electrical frequency of the drive.

At this point it should also be mentioned that the zero crossing window of phase A current, Fig. 3, has been made longer than necessary in order to illustrate the concept of the new switching technique. This extension of the zero crossing period of one phase and constant PWM of the remaining two phases will introduce lower order harmonics in the stator currents. However, in a practical implementation of a SynRM drive this zero crossing window will be much smaller than shown here because a very high frequency PWM will provide the required number of voltage pulses as shown in Fig. 5 within a very short interval and consequently the zero crossing windows can be made very small. A small zero crossing window will ensure less torque pulsations as well as insignificant lower order harmonics introduced in the stator currents. Lower order harmonics introduced because of a 200 μS window (which is enough to record the required voltage pulses using the microcontroller INTEL196KR) are insignificant compared to the fundamental component of the

TABLE I
HARMONICS IN PHASE A CURRENT

Harmonic No.	Fund./Harm(%)
2	2.5
3	2.4
4	1.6
>5	<1.5

TABLE II
HARMONICS IN PHASES B AND C CURRENT

Harmonic No.	Fund./Harm(%)
3	1.7
5	1.6
7	1.5
>9	<1.3

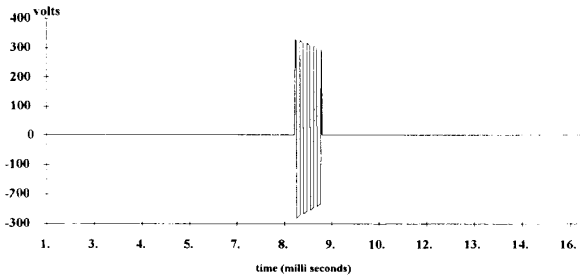

Fig. 6. Line to line induced voltage (phases A and C).

stator current which can be seen from Tables I and II giving the ratio between fundamental and harmonic currents.

The proposed technique nominally requires access to the center point of the stator of the machine. This requirement can be avoided with a simple modification of the switching technique. When the center point is not available, the controller will read the induced voltage between phase A and either of the remaining two conducting phases. It is possible to formulate the induced voltage expression similar to (14) for this modified form of switching. For the simulation the induced voltage is measured between the phases A and C and is shown in Fig. 6. Pulses of the coupled voltages shown in Fig. 6 contain the rotor position information as explained previously.

IV. STARTING ALGORITHM

It is important to note that the proposed technique can determine the rotor position even at zero speed [10]. At zero speed all phase currents are zero. This provides one with the luxury of inducing the diagnostic PWM signals on any pair of phases while the current in the other phase is controlled to experience zero current. The additional advantage is that the zero crossing can be made to persist for as long as one wishes the diagnostic interval to be. Furthermore, speed term $i_{bs}\frac{d}{dt}(L_{ab} - L_{ac})$ in (14) is eliminated in the look-up table for θ_r, which can now be derived from the simple form given below,

$$V_{\text{ind}} = (L_{ab} - L_{ac})\frac{d}{dt}i_{bs}. \tag{17}$$

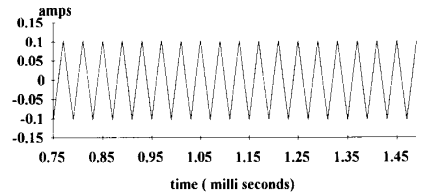

Fig. 7. Current through phase B and phase C when the induced voltage is measured across phase A at zero speed.

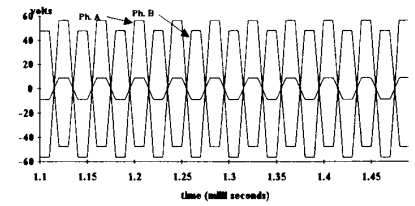

Fig. 8. Induced voltages at zero speed when the rotor is at 25 mechanical degrees.

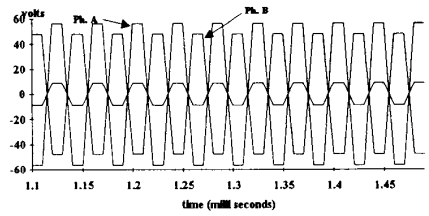

Fig. 9. Induced voltages at zero speed when the rotor is at 205 mechanical degrees.

Fig. 7 shows the diagnostic current of phases B and C during the induced voltage measurement of phase A.

To determine the rotor position uniquely, the induced voltages from all three phases have to be read. Induced voltage for phase A should be read by diagnostically energizing phases B and C. Similarly the induced voltages of phases B and C should be read by diagnostically energizing the remaining two phases. The induced voltages for three phases (when the rotor was at 25 mechanical degree) are shown in Fig. 8.

It can be noted that the phase inductances of a SynRM is a function of twice the rotor angle θ_r i.e., $2\theta_r$. Hence, for every electrical cycle the phase inductance goes through two cycles. For this reason, the induced voltages at 205 mechanical degree as shown in Fig. 9 will be the same as those shown in Fig. 8.

This apparent problem during the start-up operation has a simple solution. It does not matter for this particular case whether the algorithm picks the higher or the lower angle, because the rotor of a SynRM has no preferred polarity due to the absence of any kind of winding on the rotor. Thus, during the start-up operation the controller can be set to pick always the lower or the higher angle.

V. THE COMPLETE DRIVE SYSTEM

In order to verify key predicted results, an experimental self-synchronized SynRM drive has been implemented. The

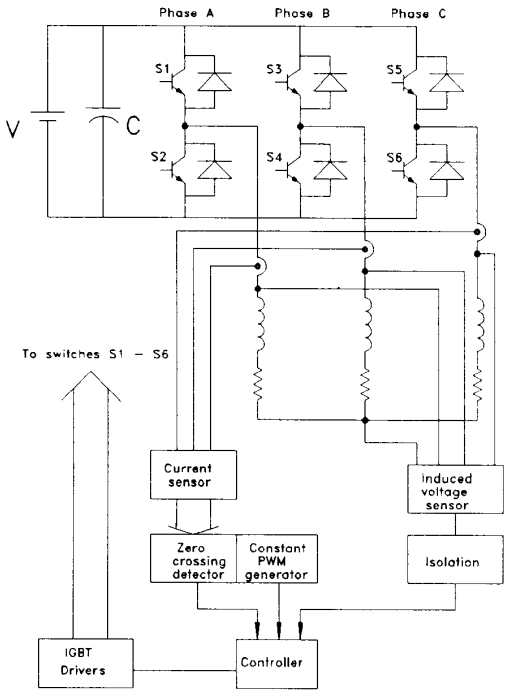

Fig. 10. Drive circuit and the control block diagram of the proposed technique.

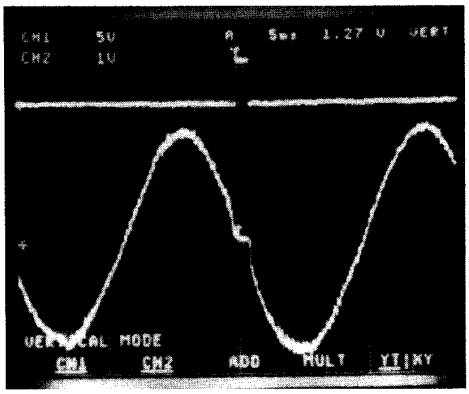

Fig. 11. Lower trace: phase A current with extended zero crossing period. Upper trace: control pulse for disconnecting phase A.

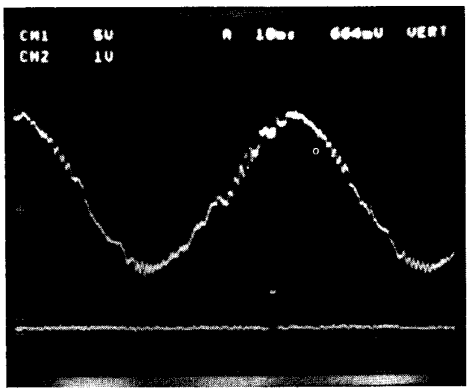

Fig. 12. Phase B current (lower trace) goes into constant PWM during the extended zero crossing of phase A.

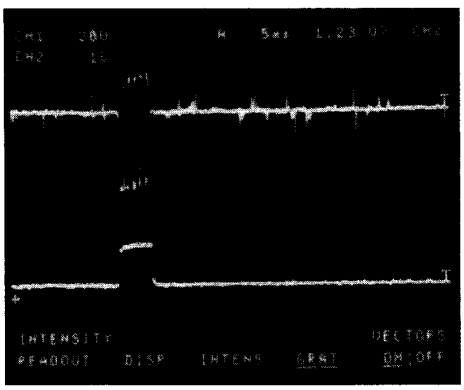

Fig. 13. Induced voltage measured in phase A. Upper trace: Induced voltage. Lower trace: control pulse.

experimental machine has an axially laminated rotor of the type described in [1]–[3]. The stator is actually a standard configuration for a 7.5 hp three-phase induction machine. The block diagram of the complete SynRM drive including the different controller segments is shown in Fig. 10. IGBT's are used as the power semiconductor devices and are driven by high voltage integrated circuit gate drivers, FUJI EXB841. The controller is configured to take the induced voltage and the phase currents and generate the gate switching signals for the three phases. The remainder of the drive system consists of the induced voltage sensing circuit which is interfaced with the phase coils. Isolation of the sensing circuit from the power circuit is accomplished by using a high frequency isolation transformer. The control algorithm routinely measures the rotor angular positions and makes the experimental drive self synchronized by advancing or retarding the phase currents.

VI. Experimental Evaluation

Throughout these tests case the SynRM operated at 1000 RPM under a lightly loaded condition. Fig. 11 shows a measured trace of the phase A current with the extended zero crossing period corresponding to Fig. 3. Note that the zero current interval is obtained, in this case only one per cycle. Fig. 12 shows the constant current PWM interval of the phase B current during that extended zero crossing period of phase A. Fig. 13 shows the induced voltage measured in phase A. Fig. 14 shows the phase A current during acceleration of the motor from rest. Note that only one zero crossing window was created at every electrical cycle of the phase current. Very good correlation with simulation, Fig. 5, is apparent. During the tests, the experimental drive was made self synchronized by advancing or retarding the phase currents depending on

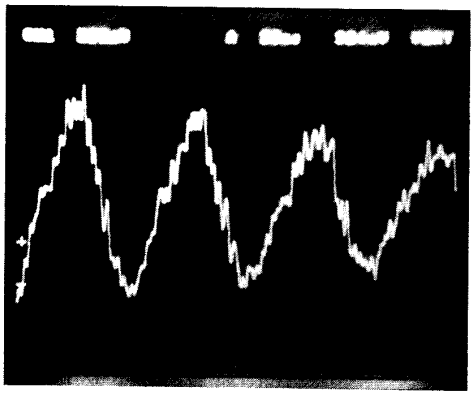

Fig. 14. Phase A current during acceleration from rest.

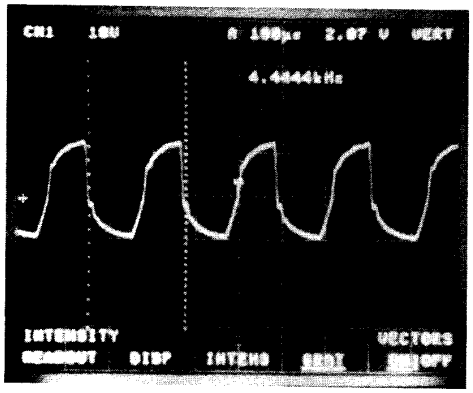

Fig. 15. Induced voltage in phase A during start up.

the rotor position. In order to calculate the starting rotor position, two phases were diagnostically energized and the induced voltage was read across the third phase. Fig. 15 shows the diagnostic constant current regulation flowing through the phases B and C of the experimental drive. Fig. 16 shows the voltage induced across phase A during this diagnostic interval. A strong, easily measurable signal is clearly evident. The accuracy of the individual rotor samples at the zero crossings of the phase currents can be obtained from the following expression [10],

$$\Delta\theta_r = \frac{\partial\theta_r}{\partial V_{\text{ind}}}\frac{V_{\max}}{2^n} + \frac{\partial\theta_r}{\partial K_1}\left(-8L_B \sin\frac{2\pi}{3} f_s \frac{I_{\max}}{2^n}\right) + \frac{\partial\theta_r}{\partial K_2}\left(-4L_B\omega_r \sin\frac{2\pi}{3}\frac{I_{\max}}{2^n}\right) \tag{18}$$

where, $\Delta\theta_r$ is the error in rotor position estimation, $V_{\max}$ is the maximum measured induced voltage, $I_{\max}$ is the maximum phase current, f_s is the PWM switching frequency during the extended zero crossing period of the phase current, and n is the number of output bits of the A/D converter. The maximum $\partial\theta_r/\partial V_{\text{ind}}$, $\partial\theta_r/\partial K_1$, and $\partial\theta_r/\partial K_2$ was found analytically maximizing them in the possible range of the three dimensions,

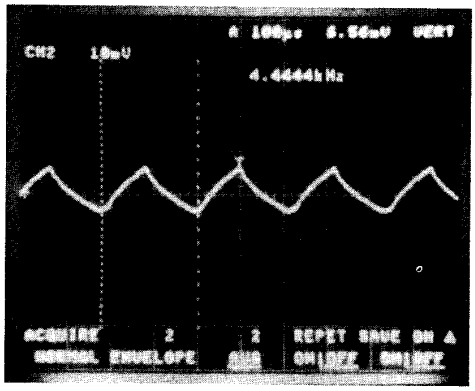

Fig. 16. Diagnostic current flowing through phases B and C during the start-up operation.

i, i^0, and V_{ind}. The worst case position error was found by substituting system parameters L_B, n, $V_{\max}$, $I_{\max}$ in (18) and the error was found to be equal to or less than 0.80 mechanical degrees. The acceleration of the drive must be,

$$K \leq 72 \cdot \Delta\theta_{\text{sample}} \cdot f_e^2 \tag{19}$$

in order to keep the estimation error between two zero crossings within $\Delta\theta_{\text{sample}}$ (here, $\Delta\theta_{\text{sample}} = 0.80$ mechanical degrees). The above mentioned analysis technique can be applied at zero speed to obtain the accuracy of the start-up rotor position estimation [9]. At zero speed the rotor position estimation error, $\Delta\theta_{\text{ro}}$, can be written as,

$$\Delta\theta_{\text{ro}} = \frac{\partial\theta_{\text{ro}}}{\partial V_{\text{ind}}}\frac{V_{\max}}{2^n} + \frac{\partial\theta_{\text{ro}}}{\partial i^0}\Delta i f_{\text{so}} \tag{20}$$

where, $i^0 \equiv di/dt$ and f_{so} is the diagnostic frequency of two stator phases when the induced voltage is measured across the remaining third phase. At zero speed, the error was found to be equal to or less than 0.50 mechanical degrees.

VII. Conclusion

A new indirect rotor position sensing method for synchronous reluctance motor drives has been presented. This measurement technique can produce smooth rotor angle data all the way to zero speed, with increasing rather decreasing accuracy. Although the proposed technique provides the rotor position information only six times in one electrical cycle, rotor positions between two zero crossings can be readily calculated using simple interpolation.

References

[1] T. A. Lipo, "Synchronous reluctance machine—A viable alternative for ac drives?" *Electric Machines and Power Syst.*, vol. 19, pp. 659–671, 1991.

[2] L. Xu, X. Xu, T. A. Lipo, and D. W. Novotny, "Vector control of a synchronous reluctance machine including saturation and iron loss," in *IEEE-IAS Conf. Rec.*, 1990, pp. 359–364.

[3] T. Matsuo and T. A. Lipo, "Field oriented control of synchronous reluctance machine," in *Proc. IEEE-PESC*, 1993, pp. 425–431.
[4] I. Boldea *et al.*, "Digital simulation of a vector controlled ALA rotor synchronous motor servo drive," *Electric Machines and Power Syst.*, vol. 19, pp. 415–424, 1991.
[5] I. Boldea *et al.*, "Torque vector control (TVC) of ALA-rotor synchronous motors," *Electric Machines and Power Syst.*, vol. 19, pp. 381–398, 1991.
[6] A. Fratta and A. Vagati, "A reluctance motor drive for high dynamic performance applications," in *Conf. Rec. IEEE-IAS*, 1987, pp. 290–293.
[7] A. J. O. Cruickshank and R. W. Menzies, "Axially laminated anistropic rotors for reluctance motors," *Proc. IEE*, vol. 113, pp. 2058–2060, 1966.
[8] P. C. Krause, *Analysis of Electric Machinery*. New York: McGraw-Hill, 1986.
[9] M. Arefeen, M. Ehsani, and T. A. Lipo, "Indirect start-up rotor position sensor for synchronous reluctance motor," *Proc. IEEE-APEC*, 1994, to be published.
[10] ——, "An analysis of the accuracy of indirect shaft sensor for synchronous reluctance motor," in *Conf. Rec. IEEE-IAS*, 1993.

M. Arefeen (S'90) received the B.S. degree in electrical engineering from Bangladesh University of Engineering and Technology, Dhaka, Bangladesh, in 1987 and the M.S. degree from Texas A&M University, College Station, TX, in 1990.

He is currently a Research Assistant in the Department of Electrical Engineering at Texas A&M University, and is working for the Ph.D. degree in the area of power electronics. His research interests are in power electronics, motor drives and their control systems.

M. Ehsani (S'70–M'81–SM'83) received the Ph.D. degree from the University of Wisconsin–Madison in 1981, in electrical engineering.

From 1974 to 1977 he was with the Fusion Research Center, University of Texas, as a Research Engineer. From 1977 to 1981 he was with Argonne National Laboratory, Argonne, IL, as a Resident Research Associate, while simultaneously doing the doctoral work at the University of Wisconsin-Madison in energy systems and control systems. Since 1981 he has been at Texas A&M University, College Station, TX, where he is now a Professor of Electrical Engineering and Director of Texas Applied Power Electronics Center (TAPC). He is the author of over 95 publications in pulsed-power supplies, high-voltage engineering, power electronics and motor drives, and is the recipient of the Prize Paper Award in Static Power Converters and motor drives at the IEEE-Industry Applications Society 1985, 1987, and 1992 Annual Meetings. In 1984 he was named the Outstanding Engineer of the Year by the Texas Society of Professional Engineers. In 1992, he was named the the Halliburton Professor in the College of Engineering at A&M. In 1994, he was also named the Dresser Industries Professor in the same college. He is the co-author of a book on converter circuits for superconductive magnetic energy storage and a contributor to an IEEE Guide for Self-Commutated Converters and other monographs. He is the author of seven U.S. patents. His current research work is in power electronics, motor drives, hybrid vehicles and their control systems.

Dr. Ehsani is a member of IEEE Power Electronics Society AdCom, Chairman of PELS Educational Affairs Committee, past Chairman of IEEE-IAS Industrial Power Converter Committee, and past Chairman of the IEEE Myron Zucker Student-Faculty Grant program. He was the General Chair of the IEEE Power Electronics Specialist Conference for 1990 and was an IEEE Industrial Electronics and Industry Applications Society Distinguished Speaker. He is also a registered professional engineer in the State of Texas.

Thomas A. Lipo (M'64–SM'71–F'87), for a photograph and biography, see this issue, p. 600.